

## Semi-Analytical Prediction of Mixed Convection in Porous Medium Using Darcy-Brinkman Model

<sup>1</sup>E. Flihi, <sup>1</sup>M. Sriti, <sup>2</sup>D. Achemlal and <sup>1</sup>M. El-Haroui

<sup>1</sup>Laboratory of Engineering Sciences, Polydisciplinary Faculty of Taza,  
Sidi Mohamed Ben Abdellah University, BP.1223 Taza, Morocco

<sup>2</sup>Laboratory of Engineering Sciences and Applications,  
National School of Applied Sciences-Al Hoceima,  
Mohammed First University, BP.03 Ajdir, Al Hoceima, Morocco

---

**Abstract:** In this research, a similarity study of mixed convection flow over a heated vertical plate embedded in Darcy-Brinkman saturated porous medium is presented. A computer code based on a fifth-order Runge-Kutta scheme with the shooting method is developed to obtain numerical solutions for resulting dimensionless governing equations. Afterward, we validated our computational code by comparing the numerical results to those obtained analytically. Subsequently, we conducted a parametric study of all parameters involved in the problem of heat transfer and flow. It is found that the increase of the mixed convection parameter, the permeability and the fluid suction reduce the thickness of the thermal boundary layer.

**Key words:** Mixed convection, Darcy-Brinkman Model, porous medium, similarity method, suction/injection, numerical results

---

### INTRODUCTION

Mixed convection flow in a porous medium saturated by a Newtonian fluid have received widespread attention due to its vast applications in many engineering and geophysical fields such as in petroleum reservoirs, geothermal reservoirs, cooling processes of nuclear reactors and thermal insulation. Many principal past studies concerning these processes can be found in the books by Ingham and Pop (2005), Neild and Bejan (2006), Pop and Ingham (2001) and Vafai (2005).

Numerous studies of such flows have been reported in the past several decades using both Darcian and non-Darcian Models for the porous medium. The Darcy law which is limited to slow flows. On the other hand, when the Reynolds number is greater than order of unity or for high velocity flow situations, Darcy's law is inapplicable because it does not account the effect of solid boundary, inertia forces. These missing effects are very significant in most practical situations such as fluid flow in geothermal reservoirs, separation processes in chemical industries, thermal insulation, petroleum reservoir and so on. These effects are incorporated by using the general flow known as Brinkman-Forchheimer extended Darcy Model. The Brinkman's extension which includes a viscous shear stress term in the momentum equation, has been used to account for the boundary

effects. The inertial effects can be modelled through the addition of a quadratic term in velocity which is known as Forchheimer's extension. Therefore, the research interest in recent studies has been focused on the important non-Darcian phenomenon of convective heat transport in porous media.

The research of Vafai and Tien (1981) presented and characterized the boundary and inertial effects in forced convective flow through a porous medium and these effects are shown to be more significant in highly permeable media, high Prandtl number fluids and in the region close to the leading edge of the flow boundary layer. A few years later, the researchers Chen *et al.* (1996) have examined the non-similar solutions for mixed convection flow along a vertical surface at different thermal conditions in porous media. In this study, the finite difference scheme was used to solve the dimensionless system of equations. It is found from this numerical investigation that the inclusion of non-Darcian effects is significantly alters the flow and heat transfer characteristics from those predicted by the traditional Darcy's Model. The non-Darcian effects investigated for a vertical plate with variable surface heat flux embedded in no-Darcian porous medium by Elbashbeshy and Bazid (2002). The results obtained indicate that the non-Darcian effects decrease the velocity and increase the temperature. On the other hand as the mixed convection

parameter increases, the dimensionless wall shear stress increases and the wall temperature decreases. After, the researchers Ishak and Nazar (2006) have studied the numerical solutions of the boundary layer flow and heat transfer over a steady and an unsteady stretching vertical surface using the Darcy-Brinkman Model. In this research, the problem is resolved numerically using the Keller-box method. The obtained results show that the surface heat transfer is increased as Pr increases and the skin friction decreases as Pr increases. Chamkha *et al.* (2011) analyzed the heat transfer by natural convection from a vertical cylinder in non-Darcian porous medium taking into account the variable viscosity of the fluid. Here, it is observed that the increase of the viscosity accelerated the fluid motion and reduced the temperature of the fluid along the wall.

Furthermore, Imran *et al.* (2012) obtained both analytical and numerical solution for an unsteady mixed convection flow of fluid through a saturated porous medium adjacent to heated/cooled semi-infinite stretching vertical sheet in the presence of heat source using the Perturbation method with Pad'e approximation for the analytical solution and the shooting method for numerical solution. The researchers showed that, the velocity and temperature decrease with an increase of the porosity of the medium and the fluid velocity increases while the temperature decreases with the increase of the mixed convection parameter Mandal and Mukhopadhyay (2013) have studied the heat transfer towards an exponentially stretching porous sheet embedded in porous medium with variable surface heat flux. These researchers found that the skin friction coefficient increases with increasing the permeability parameter as well as with the suction parameter. The characteristics of the boundary layer flow past a plane surface adjacent to a saturated Darcy-Brinkman porous medium have been investigated by Pantokratoras (2014). It has been obtained that, when the convective Darcy number increases the velocity decreases in contrast to temperature which increases and vice versa. It also found that there is a competition between the Darcy term and the Grashof term in the momentum equation and this competition makes the problem complicated.

Recently, Pantokratoras (2015) studied the forced convection in a Darcy-Brinkman porous medium with a convective thermal boundary condition. In this study, the problem has been investigated analytically as well as numerically by finite volume method. It is found that the velocity field changes from two-dimensional to one-dimensional and it is observed also that the temperature and wall heat transfer tend to an asymptotic state. This study extended the research of Achemlal *et al.* (2014) for mixed convection heat transfer along a vertical plate embedded in a porous medium, under the condition

of a variable wall temperature and a non-uniform lateral mass flux, using the Darcy-Brinkman formulation, taking into account the convective term in the momentum equation. This study finds applications in the fields of petroleum engineering, geothermal energy, etc.

### MATERIALS AND METHODS

**Mathematical formulation and resolution method:** A vertical flat plate embedded in saturated porous medium by a Newtonian fluid with applied lateral mass flux in the direction normal to the plate proportional to  $x^\lambda$  quantity is considered as shown in Fig. 1. The temperature distribution of the plate has been assumed as:

$$T_w = T_\infty + Ax^\lambda$$

Where:

- x = The distance measured along the vertical plate
- $\lambda$  = The constant temperature exponent
- $T_\infty$  = The temperature away from the plate assumed constant
- A = Positive constant

The cartesian coordinates x and y are measured, respectively, along and perpendicular to the plate. The flow is supposed two-dimensional, steady and laminar for an incompressible fluid. The convective fluid and the porous medium are supposed in local thermodynamic equilibrium anywhere and no dissipation of energy by viscosity. The fluid and medium properties are assumed constant. The boundary effects and convective term are all considered in the momentum equation.

By considering, the assumptions mentioned above, the governing equations for this model, based on the boundary layer and Boussinesq approximations are:

$$\begin{cases} \frac{\partial u}{\partial x} + \frac{\partial v}{\partial y} = 0 \\ u \frac{\partial u}{\partial x} + v \frac{\partial u}{\partial y} = \nu \frac{\partial^2 u}{\partial y^2} + g\beta(T - T_\infty) - \frac{\nu}{K} u \\ u \frac{\partial T}{\partial x} + v \frac{\partial T}{\partial y} = a \frac{\partial^2 T}{\partial y^2} \end{cases} \quad (1)$$

The associated boundary conditions are given by:

$$\begin{cases} y=0, x \geq 0, u = U_0, v = V_w, T = T_w \\ y \rightarrow \infty, x \geq 0, u = 0, T \rightarrow T_\infty \end{cases} \quad (2)$$

Where:

- u and v = The velocity components along x and y axes
- T = The temperature of Newtonian fluid

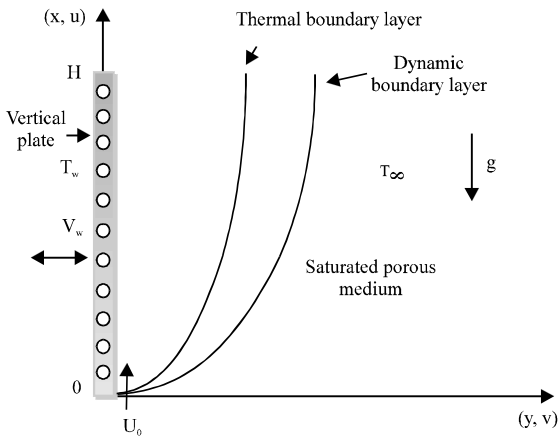


Fig. 1: Physical model and coordinate system

The constants  $\nu$ ,  $\alpha$ ,  $g$  and  $\beta$  are respectively, kinematic viscosity, thermal diffusivity, gravitational acceleration and thermal expansion coefficient.  $U_0 = ax$  and  $V_w = B.x^{(\alpha-1)/2}$  are respectively, the free stream velocity parallel to the vertical plate and the lateral mass flux, where  $B$  is a constant. The non-linearity of the model and the complexity of the phenomena encountered (boundary layer, instability, geometry of the porous medium) make difficult its resolution direct. The transformation of the PDE system, describing the problem studied in a simple non-linear differential equation becomes indispensable. So, we apply the following similarity transformations:

$$\eta = y \left( \frac{a}{\nu} \right)^{1/2}, \quad \psi = (a\nu)^{1/2} x.f(\eta), \quad \theta = \frac{T - T_\infty}{T_w - T_\infty} \quad (3)$$

where,  $\psi$  is the stream function defined in the usual notation as:  $u = \partial\psi/\partial y$  and  $v = \partial\psi/\partial x$  and  $\eta$  the similarity variable. After substitution and development, the system of Eq. 1 can be written as follow:

$$\begin{cases} f''' + ff'' - f'^2 - \frac{1}{DaRe} f' + g_s \theta = 0 \\ \theta'' + Pr(f\theta' - \lambda f'\theta) = 0 \end{cases} \quad (4)$$

where,  $g_s = Gr/Re^2$  is the mixed convection parameter,  $Gr = \beta g(T_w - T_\infty)x^3/\nu^2$  is the local Grashof number,  $Re = U_0 x/\nu$  is the local Reynolds number and  $Pr = \nu/\alpha$ ,  $Da = K/x^2$  are respectively, the Prandtl number and the local Darcy number. The transformed boundary conditions for system of Eq. 2 are:

$$\begin{cases} \eta = 0, & f(0) = f_w, & f'(0) = 1, & \theta(0) = 1 \\ \eta \rightarrow \infty, & f(\infty) = 0, & \theta(\infty) = 0 \end{cases} \quad (5)$$

where,  $f_w = -V_w(x/U_0\nu)$  is the suction/injection parameter. The system of the ordinary differential (Eq. 4) with the boundary (Eq. 5) are solved numerically by using the 5th-order Runge-Kutta scheme associated with the shooting method.

**Skin-friction coefficient and nusselt number:** The physical quantities of most interest in such problems are the local skin friction Coefficient  $C_f$  and local Nusselt number  $Nu$  which indicate physically wall shear stress and rate of heat transfer, respectively. The local skin friction coefficient and the local Nusselt number are given, respectively, by the following Eq. 6:

$$C_f = \frac{2t_w}{\rho U_0^2}, \quad Nu = \frac{x.q_w}{k(T_w - T_\infty)} \quad (6)$$

where, the skin-friction  $\tau_w$  and the heat transfer  $q_w$  at the plate surface are defined, respectively, by:

$$t_w = \mu \left( \frac{\partial u}{\partial y} \right)_{y=0}, \quad q_w = -k \left( \frac{\partial T}{\partial y} \right)_{y=0} \quad (7)$$

with  $\mu$  and  $k$  being the dynamic viscosity and thermal conductivity, respectively. Using the similarity transformations (Eq. 3) we get.

$$C_f = \frac{2}{\sqrt{Re}} f'(0), \quad Nu = -\sqrt{Re} \theta'(0) \quad (8)$$

## RESULTS AND DISCUSSION

In this study, we have analyzed the effects of the temperature exponent parameter  $\lambda$ , suction/injection parameter  $f_w$ , Prandtl number  $Pr$ , Reynolds number  $Re$ , Darcy number  $Da$  and the mixed convection parameter  $g_s$  on the mixed convection flow over a heated vertical flat plate embedded in a saturated non-Darcian porous medium. We note that the fluid suction corresponds to  $f_w > 0$ , fluid injection to  $f_w < 0$  and impermeable plate to  $f_w = 0$ . We notice that, the importance of heat transfer regime relative to the other is characterized by the mixed convection parameter  $g_s$ . The case  $g_s < 1$  corresponds to pure forced convection,  $g_s = 1$  corresponds to mixed convection and  $g_s > 1$  corresponds to pure free convection.

The comparisons are made with Imran *et al.* (2012) and Ishak and Nazar (2006) results in term of local Nusselt number and local skin friction coefficient, for some special cases (i.e., for non-porous medium and for Brinkman-Darcy porous medium) are presented in Table 1-3, showing a very good agreement.

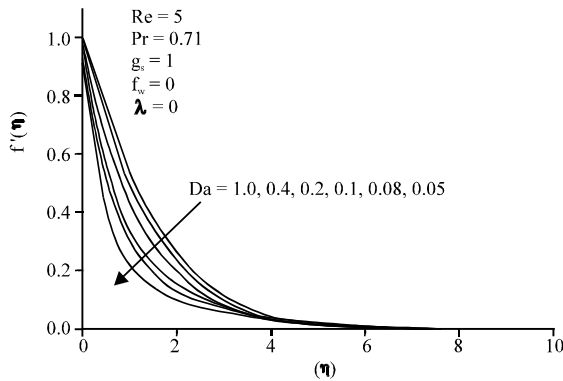


Fig. 2: Influence of Darcy number  $Da$  on the dimensionless velocity profiles for  $\lambda = 0$  and  $f_w = 0$

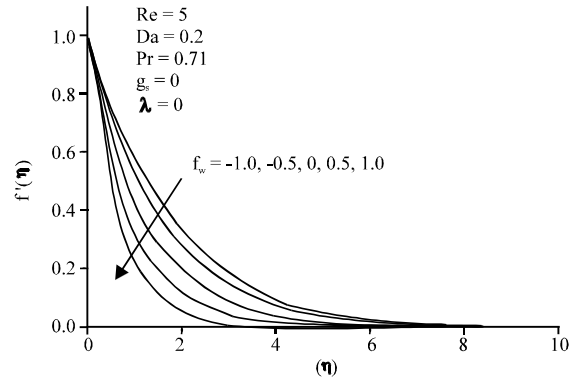


Fig. 3: Influence of parameter  $f_w$  on the dimensionless velocity profiles for  $\lambda = 0$

Table 1:  $Nu/Re^{1/2}$  for various values of  $Pr$  when  $g_s = 0$  and the infinitely permeable regime

Pr	Analytical results by Imran <i>et al.</i> (2012)	Present study numerical results	RE (%) / Imran <i>et al.</i> (2012)
0.72	0.8086	0.8088	0.020
1.00	1.0000	1.0000	0.000
3.00	1.9234	1.9236	0.010
10.0	3.7205	3.7206	0.002

Table 2:  $C_f/Re^{1/2}$  for various values of  $Da$  and  $Pr$  when  $Re = 5$ ,  $g_s = 1$ ,  $\lambda = 1$  and  $fw = 0$

Da	Pr	Results by Ishak and Nazar (2006)	Present study numerical results	RE (%) / Ishak and Nazar (2006)
0.2	0.72	-0.9625	-0.9625	0.000
0.2	1.00	-1.0000	-1.0000	0.000
0.2	6.80	-1.2089	-1.2089	0.000
0.2	10.0	-1.2404	-1.2404	0.000
0.4	0.72	-2.1118	-2.1118	0.000
0.4	1.00	-2.1281	-2.1281	0.000
0.4	6.80	-2.2584	-2.2583	0.004
0.4	10.0	-2.2848	-2.2848	0.000

Table 3:  $Nu/Re^{1/2}$  for various values of  $Da$  and  $Pr$  when  $Re = 5$ ,  $g_s = 1$ ,  $\lambda = 1$  and  $fw = 0$

Da	Pr	Results by Ishak and Nazar (2006)	Present study numerical results	RE (%) / Ishak and Nazar (2006)
0.2	0.72	0.8278	0.8278	0.000
0.2	1.00	1.0000	1.0000	0.000
0.2	6.80	2.9573	2.9571	0.006
0.2	10.0	3.6478	3.6474	0.010
0.4	0.72	0.6374	0.6373	0.010
0.4	1.00	0.7917	0.7918	0.010
0.4	6.80	2.6953	2.6952	0.003
0.4	10.0	3.3859	3.3860	0.002

**Velocity profiles:** Figure 2 shows for  $g_s = 1$  the dimensionless velocity distributions in the boundary layer area for an isothermal ( $\lambda = 0$ ) and impermeable vertical plate injected in a saturated porous medium for various values of Darcy number  $Da$ . Here, we find that the more permeable porous media permit to increase the velocity flow near the plate and consequentially expand the dynamic boundary layer thickness.

Figure 3 predicts for  $g_s = 1$ , the dimensionless velocity profiles across the boundary layer area of an isothermal ( $\lambda = 0$ ) for selected values of the suction/injection parameter  $f_w$ . From this Fig. 3, it is clearly notable that the dynamic boundary layer thickness decreases with fluid suction in increases with fluid injection and this is in agreement with the results found by Achemlal *et al.* (2014). The displayed Fig. 4 shows the dimensionless velocity profiles in the boundary layer area for an isothermal ( $\lambda = 0$ ) and impermeable plate embedded in a saturated porous medium for three convection heat transfer regimes ( $g_s < 1$ ,  $g_s = 1$ ,  $g_s > 1$ ). Here, we notice that the velocity profiles are reduced quickly in passing from the free convection heat transfer regime ( $g_s > 1$ ) to the forced convection heat transfer regime ( $g_s < 1$ ). In the other hand, the dynamic boundary layer thickness decreases with the forced convection heat transfer dominated regime and increases with the free convection heat transfer dominated regime.

**Temperature profiles:** The temperature profiles are plotted in Fig. 5 to illustrate the effect of the temperature exponent parameter  $\lambda$ . From this figure, it is observed that the temperature decreases with increasing the temperature exponent parameter.

The effect of the fluid suction/injection at the plate surface on the dimensionless temperature distributions in the boundary layer area is illustrated in Fig. 6. Here, we note that the suction of the fluid at the plate reduces the temperature profiles in the boundary layer area and consequently helps to reduce the thermal boundary layer thickness.

In Fig. 7, we present the variation of the temperature distributions for various values of  $Pr$ . It is observed that, the temperature profiles decrease as the Prandtl number increases, indicating the fact that an increase in Prandtl

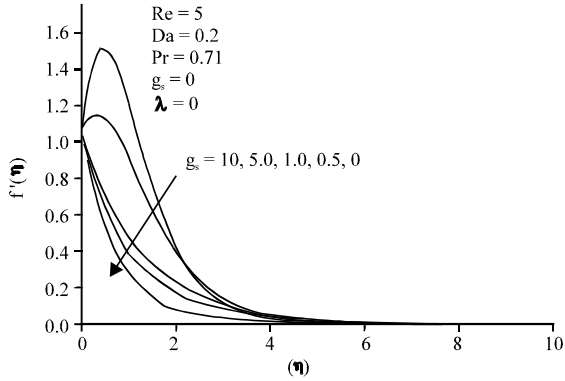


Fig. 4: Influence of parameter  $g_s$  on the dimensionless velocity profiles for  $\lambda = 0$  and  $f_w = 0$

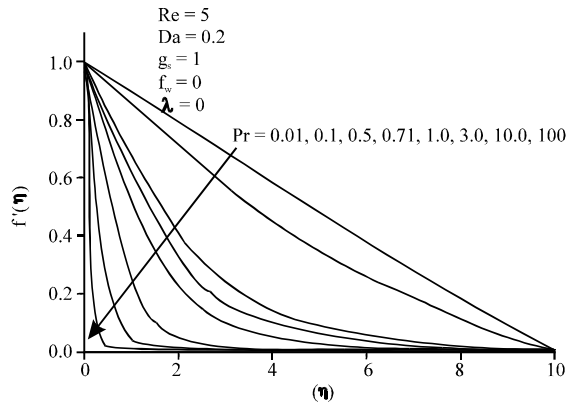


Fig. 7: Influence of Pr number on the dimensionless temperature profiles for  $\lambda = 0$  and  $f_w = 0$

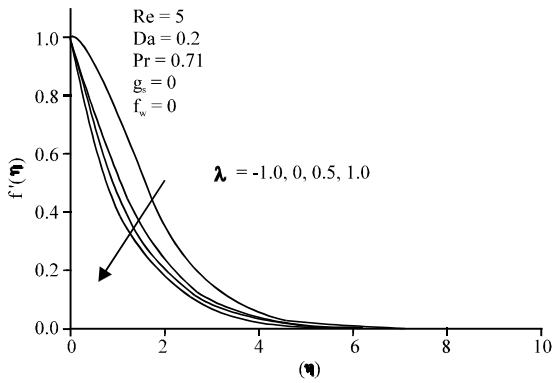


Fig. 5: Influence of parameter  $\lambda$  on the dimensionless temperature profiles for  $f_w = 0$

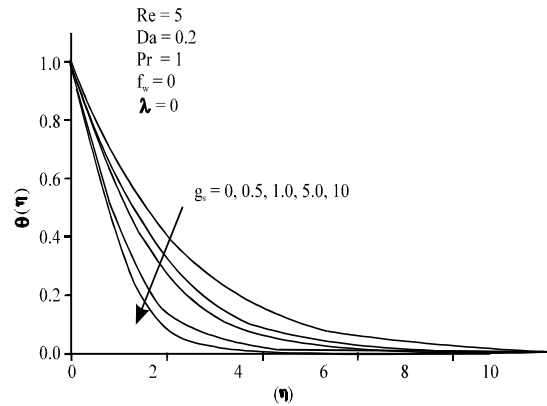


Fig. 8: Influence of parameter  $g_s$  on the dimensionless temperature profiles for  $\lambda = 0$  and  $f_w = 0$

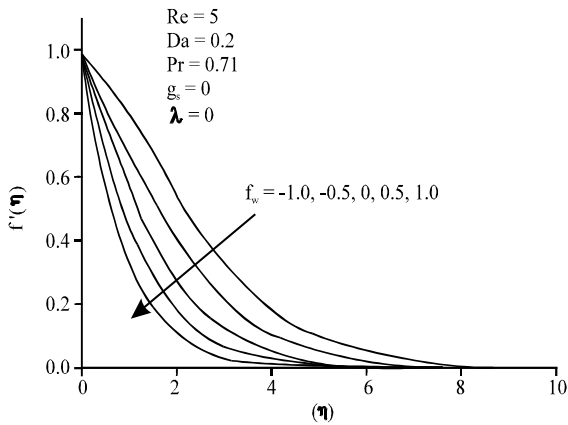


Fig. 6: Influence of parameter  $f_w$  on the dimensionless temperature profiles for  $\lambda = 0$

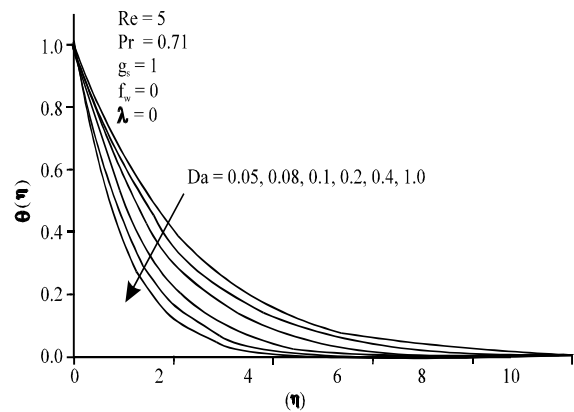


Fig. 9: Influence of Da number on the dimensionless temperature profiles for  $\lambda = 0$  and  $f_w = 0$

number reduces the thermal boundary layer thickness. The temperature profiles for various values of mixed convection parameter  $g_s$  are shown in Fig. 8. Here, it is

observed that the increase in value of  $g_s$  the temperature profiles decrease which results in a reduction of the thermal thickness boundary layer.

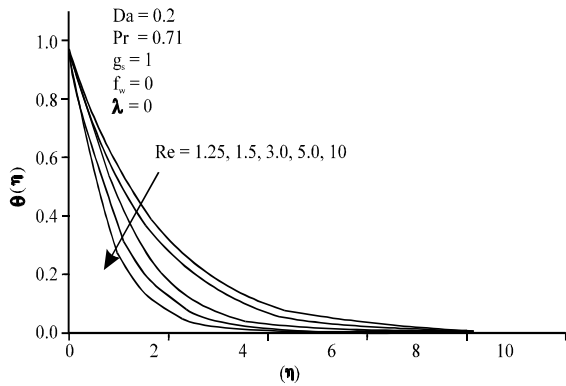


Fig. 10: Influence of number on the dimensionless temperature profiles for

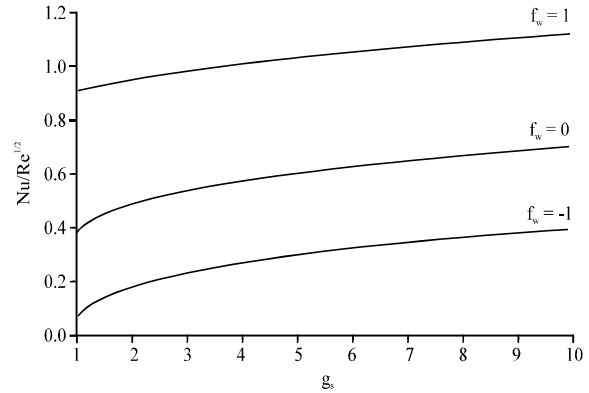


Fig. 13: Nusselt number profiles versus of parameter  $g_s$  for various values of  $f_w$

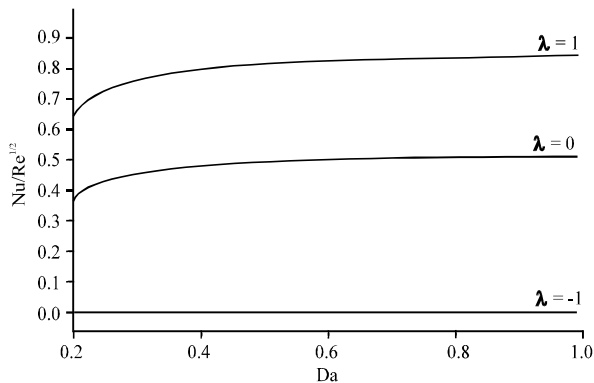


Fig. 11: Nusselt number profiles versus Darcy number  $Da$  for various values of  $\lambda$

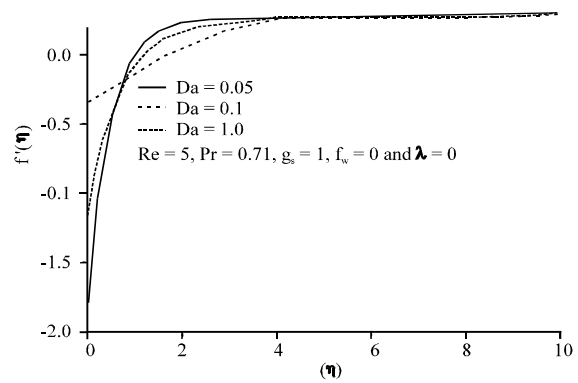


Fig. 14: Shear stress profiles for various values of Darcy number  $Da$

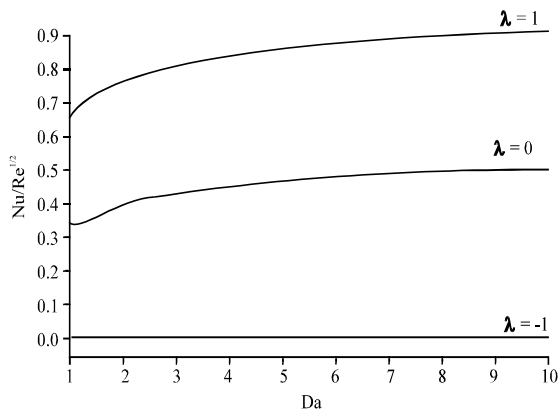


Fig. 12: Nusselt number profiles versus Reynolds number  $Re$  for various values of  $\lambda$

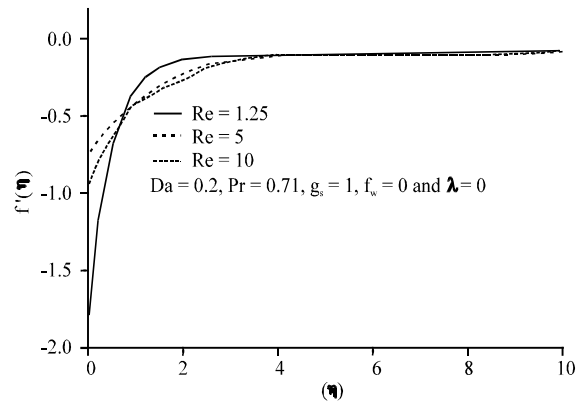


Fig. 15: Shear stress profiles for various values of Reynolds number  $Re$

Figure 9 shows the influence of the local Darcy number  $Da$  on the dimensionless temperature profiles for an isothermal and impermeable plate in the case of mixed convection. We notice that, the permeable porous

medium promotes more the cooling in the boundary layer area, which explained the reduction in the temperature profiles.

In Fig. 10, we present the temperature profiles for various values of the Reynolds number  $Re$ . We conclude

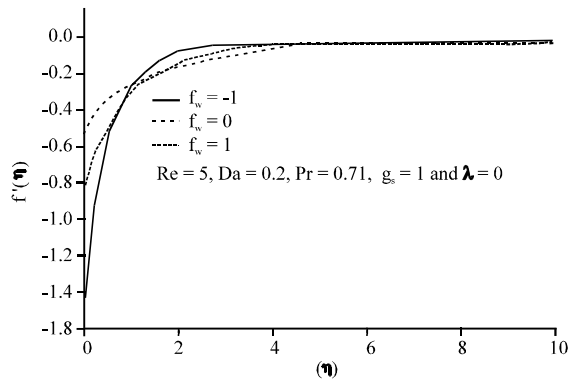


Fig. 16: Shear stress profiles for various values of parameter  $f_w$

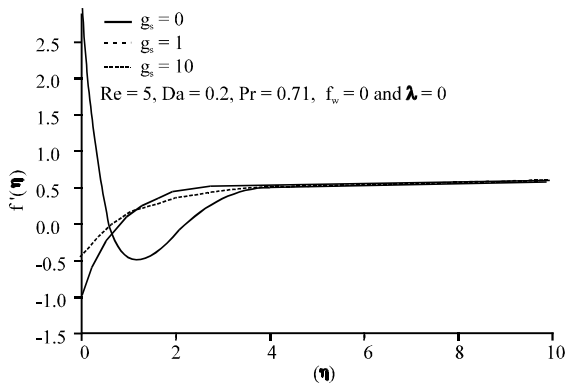


Fig. 17: Shear stress profiles for various values of parameter  $g_s$

from this figure, that the inertial forces helps to reduce the thermal boundary layer thickness unlike the effect of the shear forces which allows to expand it.

**Local nusselt number profiles:** The effects of Reynolds and Darcy number on the rate heat transfer at the wall for three thermal state of the plate surface ( $\lambda = -1, 0, 1$ ) are shown, respectively in Fig. 11 and 12. From these figures, it can be seen that increasing Re and Da leads to an increase in Nusselt number for both two cases  $\lambda = 0$  and  $\lambda = 1$ . On the other hand, for  $\lambda = -1$ , it can be noted that the rate of heat transfer remains constant and equal to zero, indicating that there is no heat exchange between the plate and the porous medium.

Figure 13 illustrates the local Nusselt number profiles according to the mixed convection parameter  $g_s$  in the case of permeable  $f_w \neq 0$  and impermeable plate  $f_w = 0$ . Here, it clearly notable that heat transfer rate is more important at the wall in passing from the forced convection regime  $g_s < 1$  to the free convection  $g_s > 1$ . In

addition, this rate is amplified with fluid suction and reduced with fluid injection. This evolution is due also to the dominance of the gravitational forces in boundary layer area.

**Local skin friction coefficient profiles:** Figure 14 shows for  $g_s = 1$ , the dimensionless shear stress profiles in the boundary layer area of an isothermal and impermeable plate for various values of the Darcy number Da. Here, it is remarkable that the frictional forces become important near the plate surface in the case where the porous medium is more permeable when compared to the case where the porous medium is less permeable. This can be explained by the effect of the flow velocity which is important close to the plate and that promotes more the shear stresses.

Figure 15 displays the dimensionless shear stress profiles in the boundary layer area of an isothermal and impermeable plate for various values of the Reynolds number Re in the case of the mixed convection regime. From this Fig. 15, we notice clearly that the minimum shear stress increases with increasing local Reynolds number. This can be physically justified by the increase of the flow velocity adjacent to the surface caused by the dominance of the inertial forces which consequently leads to increased frictional forces close to the wall.

In Fig. 16, we present for  $g_s = 1$ , the dimensionless shear stress profiles in the boundary layer area of an isothermal and impermeable plate for various values of the suction/injection parameter  $f_w$ . From this Fig. 16, it is clearly shown that the minimum of the shear forces in the boundary layer area increases with fluid injection and decreases with fluid suction. The increase can be justified by the effect of the fluid injection at the plate surface, which leads to the increase of the flow velocity near the latter and therefore promotes more the shear forces.

Figure 17 predicts the dimensionless shear stress profiles in the boundary layer area of an isothermal and impermeable plate for three convection heat transfer regimes ( $g_s < 1, g_s = 1, g_s > 1$ ). We notice that the shear forces are more important close to the wall in passing from the forced convection regime  $g_s < 1$  to the free convection  $g_s > 1$ . This trend can be explained by the rise of temperature differences in the boundary layer area which consequently leads to the dominance of the gravitational forces in comparison to the inertial forces.

### CONCLUSION

In this research, the effects of the parameters controlling the problem such as the temperature exponent

parameter  $\lambda$ , the suction/injection parameter  $f_w$ , the Prandtl number  $Pr$ , the Darcy number  $Da$ , the Reynolds number  $Re$  and the mixed convection parameter  $g_s$  on dimensionless temperature and velocity, dimensionless shear stress and local Nusselt number profiles have been examined and discussed in details. From the present numerical investigation the following conclusions may be drawn:

- The temperature decreases with increasing the temperature exponent parameter
- The fluid suction along the plate stabilizes the velocity and thermal boundary layer growth
- An increase in Prandtl number reduces the thermal boundary layer thickness
- The forced convection promotes the heat transfer in the boundary layer area
- Increasing the permeability of the porous medium ( $Da$ ) reduces (or stabilize) the thickness of the thermal boundary layer
- The inertial forces decrease the thermal boundary layer thickness

#### REFERENCES

- Achemlal, D., M. Sriti and M.E. Haroui, 2014. Numerical computation of mixed convection past a heated vertical plate within a saturated porous medium with variable permeability. *Modell. Measurement Control B*, 83: 50-66.
- Chamkha, A.J., S.M.M. El-Kabeir and A.M. Rashad, 2011. Heat and mass transfer by non-Darcy free convection from a vertical cylinder embedded in porous media with a temperature-dependent viscosity. *Int. J. Numer. Methods Heat Fluid Flow*, 21: 847-863.
- Chen, C.H., T.S. Chen, O. Cha and K. Chen, 1996. Non-darcy mixed convection along nonisothermal vertical surfaces in porous media. *Intl. J. Heat Mass Trans.*, 39: 1157-1164.
- Elbashbeshy, E.M.A. and M.A. Bazid, 2002. The mixed convection along a vertical plate with variable surface heat flux embedded in porous medium. *Appl. Math. Comput.*, 125: 317-324.
- Imran, S.M., S. Asgha and M. Mushtaq, 2012. Mixed convection flow over an unsteady stretching surface in a porous medium with heat source. *Math. Prob. Eng.*, 2012: 1-15.
- Ingham, D.B. and I. Pop, 2005. *Transport Phenomena in Porous Media*. Vol. 3, Pergamon, Oxford, Pages: 476.
- Ishak, A. and R. Nazar, 2006. Steady and unsteady boundary layers due to a stretching vertical sheet in a porous medium using darcy-brinkman equation model. *Intl. J. Appl. Mech. Eng.*, 11: 623-637.
- Mandal, I.C. and S. Mukhopadhyay, 2013. Heat transfer analysis for fluid flow over an exponentially stretching porous sheet with surface heat flux in porous medium. *Ain Shams Eng. J.*, 4: 103-110.
- Neild, D.A. and A. Bejan, 2006. *Convection in Porous Media*. 3rd Edn., Springer, USA., New York, pp: 47-48.
- Pantokratoras, A., 2014. Mixed convection in a darcy-brinkman porous medium with a constant convective thermal boundary condition. *Transp. Porous Media*, 104: 273-288.
- Pantokratoras, A., 2015. Forced convection in a darcy-brinkman porous medium with a convective thermal boundary condition. *J. Porous Media*, 18: 1-6.
- Pop, I. and D. Ingham, 2001. *Convective Heat Transfer: Mathematical and Computational Modelling of Viscous Fluids and Porous Media*. Pergamon Press, Oxford, England, UK., Pages: 647.
- Vafai, K. and C.L. Tien, 1981. Boundary and inertia effects on flow and heat transfer in porous media. *Int. J. Heat Mass Trans.*, 24: 195-203.
- Vafai, K., 2005. *Handbook of Porous Media*. 2nd Edn., CCR Press, Boca Raton, Florida, USA., Pages: 743.